Journal of Sound and Vibration 560 (2023) 117698

Contents lists available at ScienceDirect

Journal of Sound and Vibration

journal homepage: www.elsevier.com/locate/jsvi

On the zeros of three-DoF damped flexible systems

Siddharth Rath *, Shorya Awtar

Mechanical Engineering, University of Michigan, Ann Arbor, United States

ARTICLE INFO

Keywords:
Flexible system dynamics
Non-minimum phase zeros
Viscous damping
Modal decomposition
Zero loci

ABSTRACT

This paper presents an investigation of the non-minimum phase (NMP) zeros in the single input single output (SISO) transfer function of three-DoF (degrees of freedom) damped flexible linear time-invariant (LTI) systems under the assumption of classical damping. It is well-known that when all the modal residue signs of any multi-DoF damped flexible LTI system are the same, NMP zeros never occur in the system dynamics for any value of system parameters including modal residue, modal frequency and modal damping ratio. However, when all the modal residue signs are not the same, then additional conditions in terms of the system parameters are required to guarantee the elimination of NMP zeros. In this paper, the zero loci of a three-DoF damped flexible LTI system are developed to derive the sufficient and necessary conditions for the elimination of all NMP zeros. These conditions can be employed in the robust physical design of flexible systems, i.e., as long as these conditions are satisfied, the elimination of NMP zeros is guaranteed even when the system parameters undergo variations.

1. Introduction and background

Flexible system dynamics plays a vital role in the performance of several motion and vibration control applications such as space structures [1,2], rotorcraft blades [3,4], hard-disk drives [5,6], flexure mechanisms [7,8], and motion systems with transmission compliance [9,10]. These applications often require the use of feedback and feedforward control in an attempt to achieve multiple competing requirements including high speed, low settling time, strong disturbance rejection, low sensitivity to modeling uncertainties, and/or stability robustness. However, the presence of undamped poles and non-minimum phase (NMP) zero dynamics in the single input single output (SISO) transfer function lead to significant tradeoffs amongst these competing requirements. A zero is non-minimum phase (NMP) if it has a positive real component, and minimum phase (MP) if it has a non-positive real component.

One particular application that highlights the tradeoffs between the above control requirements is of flexure mechanisms used in high-precision high-speed positioning stages that exhibit lightly damped poles and NMP zeros [7,11,12]. In this application, the system zeros were analytically and experimentally shown to transition from minimum phase (MP) to non-minimum phase (NMP) as a function of parameters such as mass asymmetry and operating point. This variability in the zero dynamics makes the flexible system all the more challenging to control. In such applications of flexible systems, it is highly desirable to "guarantee" the absence of NMP zeros over the expected range of parameter variability via informed physical design. We refer to this as *robust physical design* of flexible systems.

The physical consequences of NMP zeros on control performance of flexible systems is well-documented in the literature [13–16]. For example, a real NMP zero (i.e. with imaginary component = 0) guarantees the presence of undershoot in the step response [16]. It has been experimentally shown that the undershoot due to a real NMP zero and overshoot due to undamped poles limit the response

* Corresponding author.
E-mail address: rathsid@umich.edu (S. Rath).

https://doi.org/10.1016/j.jsv.2023.117698
Received 22 August 2022; Received in revised form 20 February 2023; Accepted 30 March 2023
Available online 11 April 2023

time of a flexible one-link robot [14]. It is noteworthy that the presence of undershoot is only guaranteed for real NMP zeros; complex NMP zeros (i.e. with imaginary component $\neq 0$) may or may not lead to undershoot as numerically demonstrated in [17]. The presence of any NMP zero also leads to a tradeoff between closed-loop bandwidth and stability robustness [15]. Poor stability robustness in flexible systems leads to undesired residual vibrations, especially in case of modeling uncertainty. This is experimentally shown in [13] where the presence of complex NMP zeros in the end-point positioning control of a cantilevered beam leads to residual vibrations.

Apart from the effect of NMP zeros on the control performance of flexible systems, these zeros are also linked to the vibration performance of flexible systems. Recent investigation in the dynamics of flexure mechanisms revealed that complex NMP zeros and mode localization occur together for the same values of physical parameters [12]. These two phenomena concurrently occur in flexible systems that exhibit closely spaced modes arising from their periodic structure as well as small parametric asymmetry. It is well-known that mode localization is responsible for localized vibration in large space structures and turbine blades which leads to their premature failure [18–20]. The above-noted correlation between complex NMP zeros and mode localization can offer a means to predict and eliminate mode localization, which can be of significant value in these applications. Furthermore, Mottershead [21] numerically demonstrated the presence of complex NMP zeros in multi-DoF flexible systems and showed that in open-loop response, vibration is not completely eliminated at the frequency of these zeros. Furthermore, Mottershead [22,23] has shown that zeros of multi-DoF flexible systems placed on the imaginary axis exhibit no vibration at these zero frequencies. However, these papers do not demonstrate how complex NMP zeros can be moved to zeros on the imaginary axis.

These undesirable physical consequences of NMP zeros on the control and vibration performance of flexible systems motivate the need to systematically and comprehensively investigate the relationship between NMP zeros and the system parameters. Such an understanding can inform the design of flexible systems to intentionally eliminate NMP zeros.

Rath [24] provides a comprehensive review of the research literature on zeros of linear time-invariant (LTI) flexible systems, dating back to the 1980s. This review reveals that comprehensive sufficient and necessary conditions for the elimination of NMP zeros had not been reported in the literature for damped LTI flexible systems. Furthermore, Rath [24] investigated the zeros of a three-DoF (Degrees of Freedom) *undamped* flexible LTI system by employing modal decomposition of the SISO transfer function. Five different zero types were investigated – complex MP (CMP) i.e. imaginary component $\neq 0$, real MP (RMP) i.e. imaginary component $= 0$, marginal MP (MMP) i.e. real component $= 0$, complex NMP (CNMP), and real NMP (RNMP). Comprehensive sufficient and necessary conditions were then derived in terms of the system parameters, i.e. modal residues and frequencies, to guarantee the elimination of all NMP zeros. But this investigation did not consider any damping.

There is a well-established body of research on the effect of passive viscous damping on the poles of flexible systems [25–32] but less so on the zeros [33–40], even though zeros also play an important role in the dynamic performance of the flexible systems as noted above. Pang [33] analytically studied the effect of distributed viscous damping on the migration of zeros specifically for transverse vibration of an Euler-Bernoulli beam and showed that the zeros lie on the LHS of the imaginary axis. However, this study was only limited to a collocated transfer function for the specific system studied. This paper provided no commentary on whether the conclusions reached are applicable to any general collocated transfer function. Alberts [34] also analytically investigated the effect of distributed viscous damping on non-collocated transfer functions for transverse vibration of Euler-Bernoulli beams and reported the existence of NMP zeros. Duffour [35] analytically investigated the zero dynamics of two- and three- DoF flexible systems with and without damping. However, this paper did not explore the complete parameter space of the flexible systems. Hoagg [36] numerically demonstrated the presence of CNMP zeros in the non-collocated transfer function of a three-DoF damped flexible system for large value of damping ratio ($\zeta > 1.3$). These prior numerical and analytical investigations provide examples of specific flexible systems where NMP zeros are either present or absent in the presence of viscous damping. However, no general insights or conditions for the elimination of NMP zeros are provided.

Lin [37,38] studied the zeros of general multi-DoF damped flexible systems, and reported a sufficient condition for the elimination of only NMP zeros. This sufficient condition stated that collocated transfer functions will guarantee the elimination of NMP zeros in flexible systems with any viscous damping. However, this sufficient condition does not address the zeros of non-collocated transfer functions. Williams [39], under the additional assumption of classical damping, derived another sufficient condition for collocated as well as non-collocated transfer functions: If all the modal residue signs are positive and all the poles are underdamped, then all the zeros will be CMP. Compared to this, Rath [40] provided a broader sufficient condition for any level of classical damping (underdamped, critically damped, or over-damped): If all the modal residue signs are the same, then the zeros of collocated as well as non-collocated transfer functions are guaranteed to be minimum phase (RMP or CMP).

However, when all the modal residue signs are not the same, finding the sufficient and necessary conditions for elimination of NMP zeros becomes far more complex. Sufficient and necessary conditions for the elimination of NMP zeros have only been reported for two-DoF damped flexible systems [40]. To the best of the authors' knowledge, there are no previously reported conditions for three-DoF damped flexible systems, even though these systems are common and effective as reduced-order models in investigating the dynamics of practical multi-DoF flexible systems. For example, Tohyama [41,42] studied the zero dynamics of a transfer function associated with room acoustics, which is an infinite DoF system, using a three-DoF flexible system model to predict the occurrence of NMP zeros. Similarly, Duffour [35] investigated the self-excited instability in brake-disk like mechanical systems in the presence of frictional contact by approximating the dynamics of the flexible system using three-DoF linearized models.

Accordingly, this paper investigates the sufficient and necessary conditions for the elimination of NMP zeros in three-DoF damped flexible systems, when all modal residue signs are not the same. Similar to previous work [39,40], we assume classical damping, which has widespread application in engineering practice because of its conceptual simplicity and practical utility [43–45]. Section 2 demonstrates how this assumption enables modal decomposition of the system transfer function, leading to the subsequent investigation into zeros. The first novel contribution of this paper, presented in Section 3, explicitly provides the sufficient and necessary conditions for the elimination of NMP zeros in terms of system parameters (i.e. modal residues, frequencies, and damping ratios) using

zero loci. Section 3 also provides several observations and inferences about the behavior of zero dynamics for this system. While the authors have used the mathematical tools of modal decomposition and zero loci previously [24,40], the addition of damping to a three-DoF flexible system makes the mathematical analysis considerably more involved and the ensuing conditions richer. This is evident from the fact that it takes three zero loci for a two-DoF damped flexible system [40] and eight zero loci for a three-DoF *undamped* flexible system [24] to derive the sufficient and necessary conditions, in contrast to the sixteen zero loci in this paper for the three-DoF damped flexible system, as shown in Section 3. The second novel contribution is in Section 4, which provides a step by step procedure that employs the above-derived conditions to determine location and values of viscous damping so as to robustly eliminate NMP zeros in a three-DoF flexible system, leading to better control and vibration performance. Finally, Section 4 provides conclusion and future research directions.

2. Zero dynamics and modal decomposition

Consider the equations of motion of a multi-DoF viscously damped flexible system given by:

$$\begin{aligned} &[\mathbf{M}]_{n\times n}\ddot{w} + [\mathbf{C}]_{n\times n}\dot{w} + [\mathbf{K}]_{n\times n}w = [\mathbf{B}]_{n\times 1}F \\ &q = [\mathbf{D}]_{1\times n}w \end{aligned} \tag{1}$$

where, [**M**], [**C**], and [**K**] denote the mass, damping, and stiffness matrices, respectively; F denotes the force acting on the system through an input vector [**B**]; and, q is the measured displacement and is a linear combination, captured by sensor vector [**D**], of the individual DoF displacements denoted by w.

If the [**M**], [**C**], and [**K**] matrices satisfy the following Caughey and O'Kelly criterion [46], the flexible system is referred to as "classically damped" system.

$$[\mathbf{C}][\mathbf{M}]^{-1}[\mathbf{K}] = [\mathbf{K}][\mathbf{M}]^{-1}[\mathbf{C}] \tag{2}$$

This classically damped modeling assumption is commonly used in engineering applications because of its conceptual and mathematical simplicity [43–45]. The natural modes of vibration (i.e. eigenvectors) of such a classically damped flexible system are real valued and exactly same as those of the corresponding undamped flexible system (when [**C**] = 0). Due to this assumption, the mode shapes matrix [**ψ**] is used to diagonalize the [**M**], [**C**] and [**K**] matrices simultaneously to obtain modal mass (m_i^{modal}), modal damping (c_i^{modal}), and modal stiffness (k_i^{modal}), as follows:

$$\begin{aligned} &[\boldsymbol{\psi}]^{\mathrm{T}}[\mathbf{M}][\boldsymbol{\psi}] = \operatorname{diag}\left(m_1^{\text{modal}}, \ldots\ldots, m_n^{\text{modal}}\right), [\boldsymbol{\psi}]^{\mathrm{T}}[\mathbf{C}][\boldsymbol{\psi}] = \operatorname{diag}\left(c_1^{\text{modal}}, \ldots\ldots, c_n^{\text{modal}}\right) \\ &[\boldsymbol{\psi}]^{\mathrm{T}}[\mathbf{K}][\boldsymbol{\psi}] = \operatorname{diag}\left(k_1^{\text{modal}}, \ldots\ldots, k_n^{\text{modal}}\right) \end{aligned} \tag{3}$$

The SISO transfer function of this system can then be modally decomposed, i.e., written as the sum of n second order modes [47], as follows:

$$G(s) = \frac{q(s)}{F(s)} = \sum_{i=1}^{n} \frac{\alpha_i}{s^2 + 2\zeta_i\omega_i s + \omega_i^2} \tag{4}$$

where,

$$\alpha_i = \frac{\left([\mathbf{D}][\boldsymbol{\psi}]\right)_i \left([\boldsymbol{\psi}]^{\mathrm{T}}[\mathbf{B}]\right)_i}{m_i^{\text{modal}}}, \zeta_i = \frac{c_i^{\text{modal}}}{2\sqrt{m_i^{\text{modal}} k_i^{\text{modal}}}}, \omega_i = \sqrt{\frac{k_i^{\text{modal}}}{m_i^{\text{modal}}}} \tag{5}$$

The total number of second order modes (n) in the modal decomposition of $G(s)$ is equal to the number of DoF of the flexible system. The roots of each second order mode in Eq. (4) lie on the LHS of the imaginary axis due to the presence of positive viscous damping. Each second order mode is characterized by three real valued system parameters namely, modal residue (α_i), modal frequency (ω_i), and modal damping ratio (ζ_i). The modal residue (α_i) can be expressed in terms of the input vector [**B**], which depends on actuator location, and the sensor vector [**D**], which depends on sensor location, as well as the mode shapes matrix ([**ψ**]), as shown in Eq. (5). The columns of the matrix [**ψ**] are the mode shape vectors of the flexible system. Similarly, the modal damping ratio (ζ_i) and modal frequency (ω_i) can be expressed in terms of the modal damping, mass, and stiffness.

In this paper, we use a set of mathematical and graphical tools, namely modal decomposition (as noted above) and zero loci (presented in Sections 3), to generate granular insights into the behavior of different types of zeros as a function of system parameters (α_i, ω_i, and ζ_i). We are able to differentiate between different types of NMP zeros, and provide separate conditions to eliminate each specific type, e.g. all NMP zeros, or CNMP zeros only, or RNMP zeros only. For example, **Result 1** in Section 3 provides sufficient conditions for the elimination of *CNMP zeros* in a three-DoF damped flexible system, while **Result 3** provides sufficient and necessary conditions for the elimination of *all NMP zeros* in such a system. The graphical insights also allow us to examine the robustness of the zero dynamics to parametric variations i.e. how close the zeros are to the imaginary axis where they can transition from minimum phase to non-minimum phase.

Thus, the conditions for elimination of various types of NMP zeros derived in this paper, in terms of the system parameters, help inform physical design choices such as selection of viscous damping strategies and magnitude i.e. choice of [**C**], actuator and sensor placement i.e. choice of [**B**] and [**D**], mass and stiffness distribution i.e. choice of [**M**] and [**K**]. The relation between these systems parameters (α_i, ω_i, and ζ_i) and the physical design choices ([**M**], [**C**], [**K**], [**B**] and [**D**]) are given by Eq. (3) and Eq. (5). Physical design choices, thus informed, can lead to robust physical designs that guarantee the elimination of NMP zeros over a wide range of system parameters.

As discussed in Section 1, according to the sufficient conditions provided in [39,40] when all the modal residue signs are the same, the zeros of the transfer function of a multi-DoF damped flexible system given by Eq. (4) will always be minimum phase. Therefore, in the subsequent section, in order to derive the sufficient and necessary conditions for the elimination of NMP zeros, we will only consider the cases where all the modal residue signs are not the same.

3. Three-DOF damped flexible systems

The SISO transfer function of a three-DoF classically damped flexible system is given by $G_3(s)$:

$$G_3(s) = \frac{\alpha_R}{s^2 + 2\zeta_R\omega_R s + \omega_R^2} + \frac{\alpha_u}{s^2 + 2\zeta_u\omega_u s + \omega_u^2} + \frac{\alpha_v}{s^2 + 2\zeta_v\omega_v s + \omega_v^2}$$

where $\omega_R < \omega_u < \omega_v$. Two additional assumptions are made here. The natural frequency and damping ratio of the first flexible mode, ω_R and ζ_R, are assumed low enough to be set to zero. In previous experimental [11] and modeling work [12], CNMP zeros were reported in systems that have a low frequency rigid-body mode and at least two high frequency closely-spaced modes i.e. $\omega_R << \omega_u \approx \omega_v$. The CNMP zeros occurred very close to the frequency of the closely-spaced modes, much higher that the rigid-body mode. Furthermore, in many flexible systems damping is relatively low [26]. Thus, at the higher frequencies of interest where CNMP zeros are likely to occur, the '$\omega_R{}^2$' and the '$2\zeta_R\,\omega_R\,s$' terms can be ignored in comparison to the 's^2' term in the first mode. Motivated by practical examples [11, 12,14], these additional approximations help limit the complexity of the mathematical and graphical analysis in this section, which makes them more useful for physical system design.

Accordingly, the three-DoF damped flexible system investigated in this section can be expressed as $G_3(s) =$

$$\frac{N_3(s)}{D_3(s)} = \frac{\alpha_R}{s^2} + \frac{\alpha_u}{s^2 + 2\zeta_u\omega_u s + \omega_u^2} + \frac{\alpha_v}{s^2 + 2\zeta_v\omega_v s + \omega_v^2} \tag{6}$$

Furthermore, α_R can be set to $+1$ without any loss in generality. This reduces the number of system parameters that need to be carried through the subsequent mathematical steps. The zeros of $G_3(s)$ are investigated by studying the roots of its numerator, $N_3(s)$.

$$N_3(s) = \alpha_v s^2\left[(1+\kappa)s^2 + 2\zeta_v\omega_v(\chi\eta+\kappa)s + \omega_v^2\left(\eta^2+\kappa\right)\right] + \left(s^2 + 2\zeta_u\omega_u s + \omega_u^2\right)\left(s^2 + 2\zeta_v\omega_v s + \omega_v^2\right) \tag{7}$$

where

$$\eta \triangleq \frac{\omega_u}{\omega_v}, \chi \triangleq \frac{\zeta_u}{\zeta_v}, \text{and } \kappa \triangleq \frac{\alpha_u}{\alpha_v}$$

$N_3(s)$ is expressed in a condensed form below in terms of α_v, $A_3(s)$ and $B_3(s)$.

$$N_3(s) = \alpha_v A_3(s) + B_3(s) \tag{8}$$

where

$$A_3(s) \triangleq s^2\left[(1+\kappa)s^2 + 2\zeta_v\omega_v(\chi\eta+\kappa)s + \omega_v^2\left(\eta^2+\kappa\right)\right]$$

$$B_3(s) \triangleq \left(s^2 + 2\zeta_u\omega_u s + \omega_u^2\right)\left(s^2 + 2\zeta_v\omega_v s + \omega_v^2\right)$$

A transfer function, $T_3(s) = A_3(s) / B_3(s)$, which has no physical meaning and simply serves as a mathematical tool, is defined to capture the zero locus of $G_3(s)$. The root locus of $T_3(s)$ obtained by varying α_v, gives the zero locus of $G_3(s)$. When α_v is varied from 0 to $+\infty$, the positive root locus originates at the roots of $B_3(s)$ and terminates at the roots of $A_3(s)$. When α_v is varied from $-\infty$ to 0, the negative or complementary root locus goes from roots of $A_3(s)$ to the roots of $B_3(s)$. The goal of this section is to derive the sufficient and necessary conditions to eliminate all NMP zeros from $G_3(s)$ using its zero loci. First, a set of sufficient conditions for the elimination

Table 1
Combination of modal residue signs.

Case	α_R	α_u	α_v	$\kappa(\triangleq\alpha_u/\alpha_v)$	Result
Same Signs	+	+	+	+	[40]
Alternating Signs	+	−	+	−	**1,3**
Non-Alternating Signs	+	+	−	−	**2,4**
	+	−	−	+	

of only CNMP zeros is derived in **Results 1** and **2**, followed by the sufficient and necessary conditions for the elimination of CNMP and RNMP zeros i.e. all NMP zeros in **Results 3** and **4**.

Table 1 shows all the possible modal residue signs for a three-DoF flexible system. The case when all the modal residues are positive has already been covered in [40]. In this section, the zero dynamics will be investigated for the remaining combinations (i.e. alternating signs and non-alternating) of modal residue signs.

Zeros of $G_3(s)$ are found by setting the numerator $N_3(s)$ in Eq. (8) to zero:

$$N_3(s) = \alpha_v A_3(s) + B_3(s) = 0 \Rightarrow \alpha_v = -\frac{B_3(s)}{A_3(s)} \tag{9}$$

A few key observations can be made here. Every point on the real axis of the s-plane (i.e. $y = 0$) is always a solution of Eq. (9). When $s = x$, the RHS of Eq. (9) i.e. $B_3(s)$ / $A_3(s)$ is always a scalar with either a positive or negative sign. This means that for some positive or negative value of α_v, this equation will always be true. Therefore, the entire real axis is part of the root locus. There exists a critical value of α_v referred to as α_v^∞ for which the root locus flips from the negative real axis to the positive real axis, or vice versa by passing through infinity. This corresponds to the transition of the RMP zero of $G_3(s)$ into its RNMP zero, or vice versa. Mathematically, this condition corresponds to a loss in order of $N_3(s)$, and therefore α_v^∞ can be derived by setting the coefficient of s^4 in $N_3(s)$, given in Eq. (7), to zero.

$$\alpha_v^\infty = -\frac{1}{1+\kappa} \tag{10}$$

While the entire real axis of the s-plane is part of the root locus, only certain points on the imaginary axis can be part of the root locus. These points can be determined by applying the angle condition to Eq. (9), rearranging the terms, taking tangent on both sides, and setting $s = jy$.

$$\begin{aligned}
&(\angle B_3(s) - \angle A_3(s)) = m180^o (m \text{ is any integer})\\
&\tan(\angle B_3(s))_{s=jy} = \tan(m180^o + \angle A_3(s))_{s=jy}\\
&\Rightarrow \tan(\angle B_3(s))_{s=jy} = \tan(\angle A_3(s))_{s=jy}\\
&\Rightarrow y\left(ay^4 + by^2 + c\right) = 0\\
&\text{where } \; a \triangleq \kappa\eta(2\zeta_v\omega_v)\left(\frac{1}{\kappa\eta} + \chi\right),\; c \triangleq \frac{\kappa}{\eta^3}\left(2\zeta_v\omega_u^4\omega_v\right)\left(\frac{\eta^3}{\kappa} + \chi\right)\\
&b \triangleq \left(4\zeta_v\omega_u^2\omega_v\right)\left(\lambda\zeta_v^2 - \delta\right),\; \lambda \triangleq 2\chi\left(\frac{\kappa}{\eta} + \chi\right), \text{and } \; \delta \triangleq \frac{\kappa}{\eta}\left(\frac{\eta}{\kappa} + \chi\right)
\end{aligned} \tag{11}$$

Eq. (11) can have five real solutions in y, which correspond to five potential locations where the root locus of $T_3(s)$ intersects the imaginary axis. Note that $y = 0$ is always a solution to Eq. (11), which means that the root locus always passes through the origin of the s-plane. This is to be expected since $s = 0$ is also a root of $A_3(s)$, which corresponds to the root locus location for $\alpha_v = \pm\infty$. The other locations where the root locus crosses the imaginary axis correspond to the non-zero real solutions in y of Eq. (11). The mathematical conditions for which such crossings may or may not exist are given by:

$$\begin{aligned}
&\text{Condition I}: \; b^2 - 4ac < 0\\
&\text{Condition II}: \; b^2 - 4ac \geq 0 \;\; \text{AND} \;\; \frac{-b + \sqrt{b^2 - 4ac}}{2a} < 0\\
&\text{Condition III}: \; b^2 - 4ac \geq 0 \;\; \text{AND} \;\; \frac{-b - \sqrt{b^2 - 4ac}}{2a} < 0
\end{aligned} \tag{12}$$

Given the fourth order polynomial in Eq. (11), the root locus can cross the imaginary axis at a maximum of two sets of conjugate locations. Each set of conjugate location has a corresponding α_v that are referred to as α_{v1}^{img} and α_{v2}^{img}. The value of α_{v1}^{img} and α_{v2}^{img} when the root locus crosses the imaginary axis can be found by setting $s = jy$ in the expression for $N_3(s)$ in Eq. (7) and equating $N_3(s)$ to 0.

$$\alpha_{v1}^{\text{img}} = \frac{\omega_u\omega_v(\chi+\eta)-(1+\chi\eta)y_1^2}{(\chi\eta+\kappa)y_1^2} \quad \text{where} \quad y_1^2 = \frac{-b+\sqrt{b^2-4ac}}{2a}$$
$$\alpha_{v2}^{\text{img}} = \frac{\omega_u\omega_v(\chi+\eta)-(1+\chi\eta)y_2^2}{(\chi\eta+\kappa)y_2^2} \quad \text{where} \quad y_2^2 = \frac{-b-\sqrt{b^2-4ac}}{2a} \tag{13}$$

If Condition I is true OR [Condition II AND Condition III] are true, then there are no non-zero real solutions in y. If Condition I is not true, AND Condition II is not true AND Condition III is true, then the root locus will cross the imaginary axis at one set of conjugate locations given by $s = \pm jy_1$ and corresponding $\alpha_v = \alpha_{v1}{}^{\text{img}}$. If Condition I is not true, AND Condition II is true AND Condition III is not true, then the root locus will cross the imaginary axis at one set of conjugate locations given by $s = \pm jy_2$ and corresponding $\alpha_v = \alpha_{v2}{}^{\text{img}}$. If Condition I is not true, AND [both Condition II AND Condition III] are also not true, then the root locus will cross the imaginary axis at two sets of conjugate locations given by $s = \pm jy_1$ (corresponding $\alpha_v = \alpha_{v1}{}^{\text{img}}$) and $s = \pm jy_2$ (corresponding $\alpha_v = \alpha_{v2}{}^{\text{img}}$). Thus, the above conditions determine the number of instances where the root locus crosses the imaginary axis, which in turn informs the shape of the root locus. These crossings can happen for positive or negative values of α_v i.e. $\alpha_{v1}{}^{\text{img}}$ and $\alpha_{v2}{}^{\text{img}}$ can either be positive or negative. The detailed derivation of when $\alpha_{v1}{}^{\text{img}}$ and $\alpha_{v2}{}^{\text{img}}$ are positive or negative can be found in [48].

Having addressed how the root locus of $T_3(s)$, or equivalently the zero locus of $G_3(s)$, interacts with the real and imaginary axes of the s-plane, we next proceed to divide the parameter space, reduce the conditions from Eq. (12) to parameter ranges, and plot the resulting zero loci for various combination of parameter ranges. The steps are as follows:

1 The parameter space of the modal residues ratio i.e. κ is divided into $(\kappa < -1)$, $(-1 < \kappa < -\eta^2)$, $(-\eta^2 < \kappa < 0)$ and $(\kappa > 0)$. These four ranges span all values of κ from $-\infty$ to $+\infty$ and they were used for the analysis of NMP zeros in the analogous three-DoF *undamped*

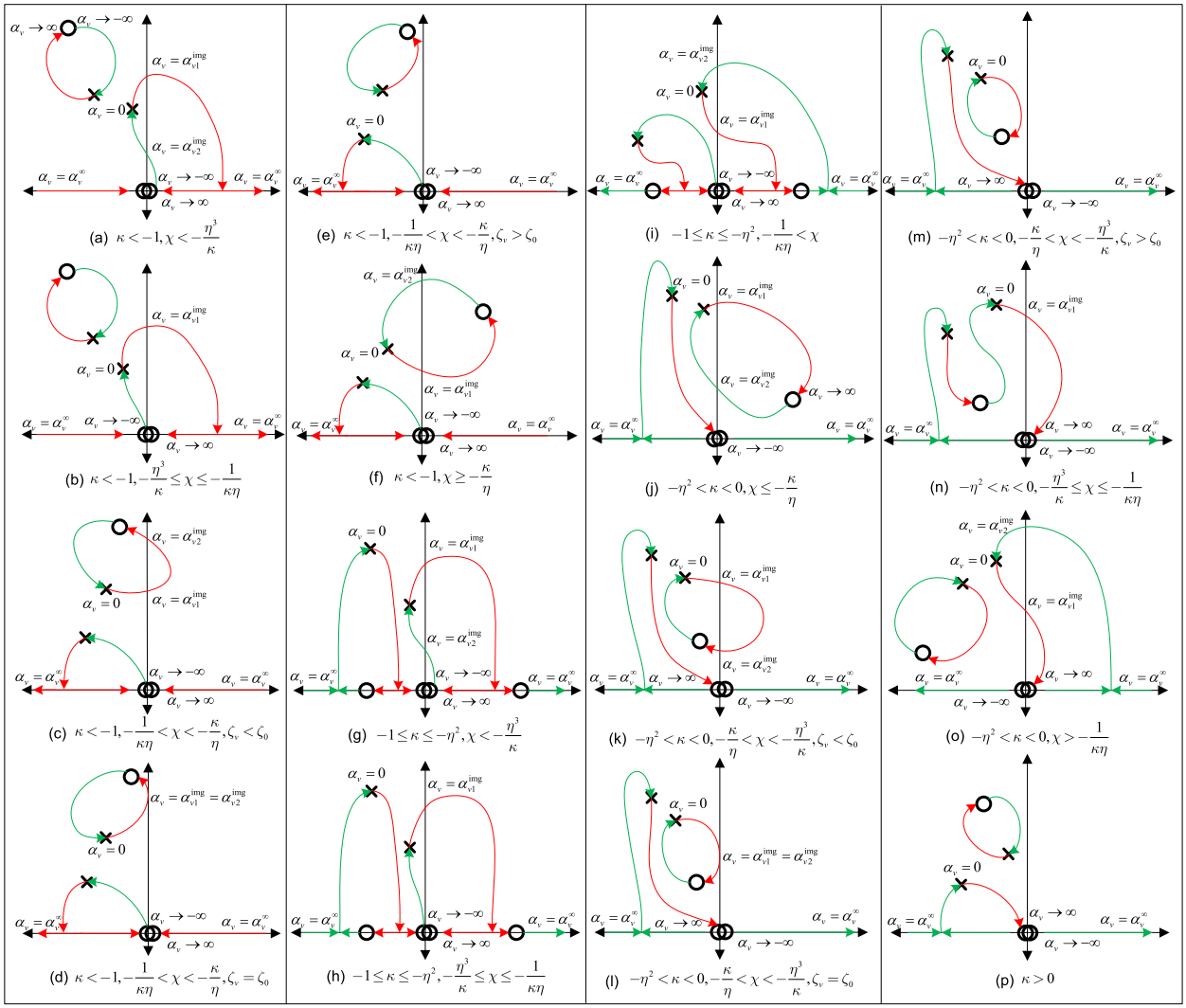

Fig. 1. Zero Loci of G $_3$ (s) for different ranges of κ, χ and ζ_v as α_v varies from $-\infty$ to 0 (green curve) and 0 to $+\infty$ (red curve). The parameter ranges of κ, χ and ζ_v are given below each sub figure.

flexible system [24]. Using the same parameter ranges of κ in this paper allows for a direct comparison between the NMP zero dynamics of the *undamped* and damped systems. This leads to inferences on how the addition of damping changes the zero loci and the resulting condition for the elimination of NMP zeros. These inferences are discussed in **Result 1** and **Result 2**.

2 The mathematical inequalities given by Condition I, Condition II, and Condition III are solved separately for all four parameter ranges of κ. This gives the non-overlapping parameter ranges of χ and ζ_v for each parameter range of κ where these conditions are or are not satisfied. These ranges are then used to draw the multiple unique zero loci of $G_3(s)$, as shown in Fig. 1. Detailed steps on the derivation of these parameter ranges can be found in [48]. For example, the parameter space of ζ_v is divided into two parameter ranges i.e. $\zeta_v < \zeta_0$ and $\zeta_v \geq \zeta_0$ in Figs. 1c-1e. The expression for ζ_0 has been directly provided in Eq. (14). But its long derivation can be found in [48].

In each of the sub figures i.e. (a) to (p), the green curve which corresponds to the negative zero locus starts from the roots of $A_3(s)$ (represented by circle in above figure, given in Eq. (8)) as α_v starts from $-\infty$ and terminates at the roots of $B_3(s)$ (represented by cross in above figure, given in Eq. (8)) as α_v becomes equal to 0. In each of the sub figures i.e. (a) to (p), the red curve which corresponds to the positive zero locus starts from the roots of $B_3(s)$ as α_v starts from 0 and terminates at the roots of $A_3(s)$ as α_v tends to $+\infty$. The portion of the zero locus (positive or negative) that lies strictly on the right hand side (RHS) of the imaginary axis leads to NMP zeros of $G_3(s)$. The analytical expression for α_v where the zero locus crosses the imaginary axis i.e. $\alpha_{v1}{}^{img}$ and $\alpha_{v2}{}^{img}$ is given in Eq. (13). The analytical expression for α_v where the zero locus tends to $+/-\infty$ on the real axis i.e. α_v^{∞} is given by Eq. (10).

The zero loci of Fig. 1 span the entire range of all the parameters: κ ($-\infty$ to $+\infty$), χ (0 to $+\infty$), ζ_v (0 to $+\infty$), η (0 to $+\infty$), and α_v ($-\infty$ to $+\infty$). For example, when ($\kappa < -1$), there are six non-overlapping parameter ranges of χ and ζ_v that lead to six unique zero loci depicted by Figs. 1a-1f. The value of α_v ranges from $-\infty$ to $+\infty$ in each of these zero loci. Based on the Table 1, the positive zero loci in Fig. 1 will be used to find the conditions for the eliminations of NMP zeros for the case of alternating sign of modal residues ($\alpha_v > 0$). Similarly, the negative zero loci in Fig. 1 will be used to do the same for the case of non-alternating sign of modal residues ($\alpha_v < 0$). This separation of mathematical conditions between alternating and non-alternating modal residue signs is done to allow a direct comparison between the results obtained in this paper and those obtained in [24] for a three-DoF *undamped* flexible system.

3.1. Sufficient conditions for eliminating CNMP zeros

Result 1: In a three-DoF damped flexible system given by Eq. (6), when the signs of the modal residues are alternating (i.e. $\alpha_v > 0$), the ratio of modal residues (κ), ratio of modal damping ratios (χ) and modal damping ratio (ζ_v) should satisfy the following inequalities to eliminate CNMP zeros for any positive value of modal residue α_v.

$$\text{Condition}\quad 1.1 : (\kappa < -1)\text{AND}\left(-\frac{1}{\kappa\eta} < \chi < -\frac{\kappa}{\eta}\right)\text{AND}(\zeta_v \geq \zeta_0)$$

OR

$$\text{Condition}\quad 1.2 : \left(-\eta^2 < \kappa < 0\right)\text{AND}\left(-\frac{\kappa}{\eta} < \chi < -\frac{\eta^3}{\kappa}\right)\text{AND}(\zeta_v \geq \zeta_0)$$

where

$$\zeta_0 \triangleq \frac{\sqrt{(\kappa+\eta\chi)(\kappa\chi+\eta) - |\kappa+\eta\chi|\sqrt{\dfrac{(\eta^3+\kappa\chi)(1+\kappa\eta\chi)}{\eta}}}}{\sqrt{2\chi}|\kappa+\eta\chi|} \tag{14}$$

Condition 1.1 is derived from Figs. 1d-1e. It can be seen that when the parameter ranges of κ, χ, and ζ_v in Figs. 1d-1e are satisfied, the positive zero loci (i.e. the red curve) do not cross the imaginary axis. Hence, for these parameter ranges, $G_3(s)$ does not exhibit CNMP zeros. Similarly, Condition 1.2 is derived from Figs. 1l-1m. When Condition 1.1 and Condition 1.2 are not met, Figs. 1a-1c, 1f-1k, and 1n-1o depict the positive zero loci crossing the imaginary axis at non-zero frequencies, indicating the presence of CNMP zeros.

Based on **Result 1** and the positive zero loci ($\alpha_v > 0$) in Fig. 1, the following observations can be made about the CNMP zero dynamics of the damped three-DoF damped flexible system:

1 Each of the conditions given in **Result 1**, i.e. Condition 1.1 and Condition 1.2, is individually sufficient for the elimination of CNMP zeros. Also, these sufficient conditions are not unique or necessary. Even when these sufficient conditions are not satisfied, Fig. 1a-1c, 1f-1k, and 1n-1o show that one can guarantee the absence of CNMP zeros by selecting ranges of α_v for which the zeros never lie on the RHS of the s-plane (excluding the RHS real axis). These ranges of α_v have been explicitly derived and reported in [48].

2 It was shown previously that for a three-DoF *undamped* flexible system with alternating modal residue signs, the sufficient and necessary condition to eliminate CNMP zeros is to tune the value of α_v such that it lies within a certain range [24]. However, as

shown in Fig. 1d, 1e, 1l, 1m and **Result 1**, the addition of viscous damping leads to sufficient conditions in terms of κ, χ, and ζ_v that guarantee the elimination of CNMP zeros for any value of α_v. Therefore, these sufficient conditions guarantee the elimination of CNMP zeros for a wider range of system parameters, especially when the modal residue α_v undergoes large variation.

Result 2: In a three-DoF damped flexible system given by Eq. (6), when the signs of the modal residues are non-alternating (i.e. $\alpha_v < 0$), the ratio of modal residues (κ) and ratio of modal damping ratios (χ) should satisfy the following mathematical inequalities to eliminate CNMP zeros for any negative value of the modal residue α_v.

$$\text{Condition } 2.1 : (\kappa < -1)\text{AND}\left(-\frac{\eta^3}{\kappa} \le \chi \le -\frac{\kappa}{\eta}\right)$$

OR

$$\text{Condition } 2.2 : \left(-1 \le \kappa \le -\eta^2\right)\text{AND}\left(-\frac{\eta^3}{\kappa} \le \chi \le -\frac{1}{\kappa\eta}\right)$$

OR

$$\text{Condition } 2.3 : \left(-\eta^2 < \kappa < 0\right)\text{AND}\left(-\frac{\kappa}{\eta} \le \chi \le -\frac{1}{\kappa\eta}\right)$$

OR

$$\text{Condition } 2.4 : (\kappa > 0)$$

Condition 2.1, Condition 2.2, Condition 2.3, and Condition 2.4 are derived from Figs. 1b-1e, Fig. 1h, Figs. 1k-1n, Fig. 1p respectively. When the parameter ranges in these conditions are satisfied, their corresponding negative zero loci (i.e. green curve) in Fig. 1 do not cross the imaginary axis at non-zero frequencies. Therefore, the absence of CNMP zeros is guaranteed. When these conditions are not met, Figs. 1a, 1f-1g, 1i-1j, and 1o depict the negative zero loci crossing the imaginary axis at non-zero frequencies, indicating the presence of CNMP zeros.

Based on **Result 2** and the negative zero loci ($\alpha_v < 0$) in Fig. 1, the following observations can be made about the CNMP zero dynamics of the damped three-DoF damped flexible system:

1 The sufficient conditions given in **Result 2** for the elimination of CNMP zeros are not unique or necessary. Even when these sufficient conditions are not satisfied, Figs. 1a, 1f-1g, 1i-1j, and 1o show that one can eliminate CNMP zeros by selecting ranges of α_v for which the zeros never lie on the RHS of the s-plane (excluding the RHS real axis). These ranges of α_v have been explicitly derived and reported in [48].
2 It was shown previously that the sequence of non-alternating modal residue signs ($\alpha_R > 0$, $\alpha_u > 0$, $\alpha_v < 0$) is a sufficient condition that guarantees the elimination of CNMP zeros for any negative value of modal residue (α_v) in a three-DoF *undamped* flexible system [24]. However, Figs. 1a, 1f-1g, 1i-1j, and 1o depict the presence of CNMP zeros for some parameter ranges of κ and χ. This shows a potential drawback of adding viscous damping to a three-DoF *undamped* flexible system. Therefore, one key advantage of the sufficient conditions in **Result 2** is that it guarantees the elimination of CNMP zeros in the presence of viscous damping even if the modal residue (α_v) undergoes large variation.
3 Condition 2.4 is derived from Fig. 1p and implies that the non-alternating modal residue signs is a sufficient condition that guarantees the elimination of CNMP zeros for any negative value of modal residue (α_v). This is unlike Conditions 2.1, 2.2, and 2.3, which also hold true for non-alternating modal residue signs, but they require additional conditions on χ to guarantee the elimination of CNMP zeros.

3.2. *Sufficient and necessary conditions for eliminating CNMP and RNMP zeros*

The sufficient conditions in **Result 1** and **Result 2** that guarantee the elimination of CNMP zeros do not guarantee the elimination of RNMP zeros. This can be seen, for example, in Figs. 1d-1e for alternating signs of modal residues and Figs. 1k-1n for non-alternating signs. In fact, in each zero locus plot of $G_3(s)$ in Fig. 1, the positive real axis is always part of the zero locus for some range of values of α_v, which confirms the presence of RNMP zeros. In this section, we will determine the sufficient and necessary conditions for eliminating CNMP *as well as* RNMP zeros such that the zeros of $G_3(s)$ always lie on or to the left of the imaginary axis. Based on Fig. 1, **Result 3** and **Result 4** provide the sufficient and necessary conditions for the elimination of all NMP zeros for alternating and non-alternating modal residue signs, respectively.

Result 3: In a three-DoF damped flexible system given by Eq. (6), when the modal residue signs are alternating ($\alpha_v > 0$), the following conditions are individually sufficient, and together necessary, to guarantee the elimination of all NMP zeros.

$$\text{Condition } 3.1: (\kappa < -1)\text{AND}\left(\chi \le -\frac{1}{\kappa\eta}\right)\text{AND}\left(\alpha_v \le \alpha_{v1}^{\text{img}}\right)$$

OR

$$\text{Condition } 3.2: (\kappa < -1)\text{AND}\left(-\frac{1}{\kappa\eta} < \chi < -\frac{\kappa}{\eta}\right)\text{AND}(\zeta_v < \zeta_0)\text{AND}\begin{pmatrix}\left\{\alpha_v \le \alpha_{v1}^{\text{img}} \text{ OR } \alpha_v \ge \alpha_{v2}^{\text{img}}\right\}\\ \text{AND}\left\{\alpha_v \le \alpha_v^{\infty}\right\}\end{pmatrix}$$

OR

$$\text{Condition } 3.3: (\kappa < -1)\text{AND}\left(-\frac{1}{\kappa\eta} < \chi < -\frac{\kappa}{\eta}\right)\text{AND}(\zeta_v \ge \zeta_0)\text{AND}\left(\alpha_v \le \alpha_v^{\infty}\right)$$

OR

$$\text{Condition } 3.4: (\kappa < -1)\text{AND}\left(\chi \ge -\frac{\kappa}{\eta}\right)\text{AND}\left(\alpha_v \le \min\left\{\alpha_{v1}^{\text{img}}, \alpha_v^{\infty}\right\}\right)$$

OR

$$\text{Condition } 3.5: \left(-1 \le \kappa \le -\eta^2\right)\text{AND}\left(\alpha_v \le \alpha_{v1}^{\text{img}}\right)$$

OR

$$\text{Condition } 3.6: \left(-\eta^2 < \kappa < 0\right)\text{AND}\left(\chi \le -\frac{\kappa}{\eta}\right)\text{AND}\left(\alpha_v \le \alpha_{v1}^{\text{img}}\right)$$

OR

$$\text{Condition } 3.7: \left(-\eta^2 < \kappa < 0\right)\text{AND}\left(-\frac{\kappa}{\eta} < \chi < -\frac{\eta^3}{\kappa}\right)\text{AND}(\zeta_v < \zeta_0)\text{AND}\left(\alpha_v \le \alpha_{v1}^{\text{img}} \text{ OR } \alpha_v \ge \alpha_{v2}^{\text{img}}\right)$$

OR

$$\text{Condition } 3.8: \left(-\eta^2 < \kappa < 0\right)\text{AND}\left(-\frac{\kappa}{\eta} < \chi < -\frac{\eta^3}{\kappa}\right)\text{AND}(\zeta_v \ge \zeta_0)$$

OR

$$\text{Condition } 3.9: \left(-\eta^2 < \kappa < 0\right)\text{AND}\left(\chi \ge -\frac{\eta^3}{\kappa}\right)\text{AND}\left(\alpha_v \le \alpha_{v1}^{\text{img}}\right)$$

Each sufficient condition in **Result 3** is derived from the positive zero loci in Fig. 1. For example, when ($\kappa < -1$) AND ($\chi < -\eta^3/\kappa$) in Fig. 1a, CNMP and RNMP zeros will not occur if $\alpha_v \le \alpha_{v1}{}^{\text{img}}$. Similarly, in Fig. 1b, when ($\kappa < -1$) AND ($-\eta^3/\kappa \le \chi \le -1/\kappa\eta$), then again CNMP and RNMP zeros will not occur if $\alpha_v \le \alpha_{v1}{}^{\text{img}}$. Therefore, combining the parameter range of χ from Fig. 1a and 1b leads to Condition 3.1 i.e. ($\kappa < -1$) AND ($\chi \le -1/\kappa\eta$) AND ($\alpha_v \le \alpha_{v1}{}^{\text{img}}$). Similarly, other sufficient conditions are also derived from the positive zero loci of Fig. 1. The correspondence between each sufficient condition and Fig.1 is as follows: Condition 3.1 → Fig. 1a and 1b, Condition 3.2 → Fig. 1c, Condition 3.3 → Fig. 1d and 1e, Condition 3.4 → Fig. 1f, Condition 3.5 → Fig. 1g, 1h and 1i, Condition 3.6 → Fig. 1j, Condition 3.7 → Fig. 1k, Condition 3.8 → Fig. 1l and 1m, and Condition 3.9 → Fig. 1n and 1o.

Based on **Result 3** and Fig. 1, the following observations can be made about the NMP zero dynamics of a three-DoF damped flexible system:

1 Each condition listed in **Result 3** is individually sufficient but not necessary. For example, Condition 3.1, by itself, is a sufficient condition. However, Condition 3.1, by itself, is not necessary because even if this condition is not met, NMP zeros can still be eliminated via other non-overlapping conditions such as Condition 3.2 or Condition 3.3.
2 Each sufficient condition comprises of parameter ranges that are essential and broadest possible. For each of these conditions, one can write various inferior conditions with narrower parameter ranges that would also be sufficient conditions. For example, based on Condition 3.1, [($\kappa < -2$) AND ($\chi \le -1/\kappa\eta$) AND ($\alpha_v \le \alpha_{v1}{}^{\text{img}}$)] is also a sufficient condition for the elimination of NMP zeros.
3 As shown by the zero loci of Fig. 1, the entire range of the system parameters comprising of modal residues, frequencies, and damping ratios is covered in this analysis. Therefore, **Result 3** is a complete list of all possible sufficient conditions. In other words, there are no other sufficient conditions for which one can guarantee the elimination of NMP zeros. As a result, these nine conditions when considered together, i.e., [Condition 3.1 OR Condition 3.2 OR Condition 3.3 OR Condition 3.4 OR Condition 3.5 OR Condition 3.6 OR Condition 3.7 OR Condition 3.8 OR Condition 3.9], form the necessary condition for the elimination of NMP zeros.
4 The mathematical form of the conditions is the consequence of our choice of parameterization. The normalized parameters κ, χ, and η that are defined in terms of system parameters and used to provide the conditions could have been defined differently. For example, instead of using α_v as the varying parameter to plot the zero locus of $G_3(s)$, one could use a different varying parameter, for example α_u. The zero locus could have been plotted as a function of modal frequencies or modal damping ratios. While the resulting mathematical form of the conditions may be different in that case, the conditions would effectively be the same in terms of system parameters. In other words, the conditions are unique.
5 The graphical visualization in Fig. 1 allows one to determine the sufficient and necessary conditions for the elimination of *specific* types of NMP zeros e.g. CNMP only, RNMP only, as well as all NMP. For example, **Result 1** provides a sufficient condition for the elimination of CNMP zeros, while **Result 3** provides sufficient and necessary conditions for the elimination of all NMP zeros. Furthermore, this graphical visualization allows one to examine the sensitivity of different types of NMP zeros to parametric variations, which helps inform

the robustness of any choice of system parameters that avoid NMP zeros. For example, when the value of α_v is close to α_{v1}^{img} in Fig. 1a, the CMP zero can flip to become a CNMP zero, and similarly when α_v is close to α_v^{∞}, RMP zero can flip to become RNMP zero in Fig. 1a.

6 Condition 3.8 is the only sufficient condition that guarantees the elimination of all NMP zeros for any positive value of modal residue, α_v or any negative value of modal residue α_u. Such a condition becomes useful in situations where the modal residues α_v or α_u undergo variations and can enable robust physical design [12]. The application of Condition 3.8 in eliminating NMP zeros is demonstrated via a case study in Section 4.

Result 4: In a three-DoF damped flexible system given by Eq. (6), when the modal residue signs are non-alternating ($\alpha_v < 0$), the following conditions are individually sufficient, and together necessary, to guarantee the elimination of all NMP zero.

$$\text{Condition } 4.1 : (\kappa < -1)\text{AND}\left(\chi < -\frac{\eta^3}{\kappa}\right)\text{AND}\left(\alpha_v \geq \alpha_{v2}^{\text{img}}\right)$$

OR

$$\text{Condition } 4.2 : (\kappa < -1)\text{AND}\left(-\frac{\eta^3}{\kappa} \leq \chi \leq -\frac{\kappa}{\eta}\right)$$

OR

$$\text{Condition } 4.3 : (\kappa < -1)\text{AND}\left(\chi > -\frac{\kappa}{\eta}\right)\text{AND}\left(\alpha_v \geq \alpha_{v2}^{\text{img}}\right)$$

OR

$$\text{Condition } 4.4 : \left(-1 \leq \kappa \leq -\eta^2\right)\text{AND}\left(\chi < -\frac{\eta^3}{\kappa}\right)\text{AND}\left(\alpha_v \geq \max\left\{\alpha_{v2}^{\text{img}}, \alpha_v^{\infty}\right\}\right)$$

OR

$$\text{Condition } 4.5 : \left(-1 \leq \kappa \leq -\eta^2\right)\text{AND}\left(-\frac{\eta^3}{\kappa} \leq \chi \leq -\frac{1}{\kappa\eta}\right)\text{AND}\left(\alpha_v \geq \alpha_v^{\infty}\right)$$

OR

$$\text{Condition } 4.6 : \left(-1 \leq \kappa \leq -\eta^2\right)\text{AND}\left(\chi > -\frac{1}{\kappa\eta}\right)\text{AND}\left(\alpha_v \leq \alpha_v^{\infty}\ \text{OR}\ \alpha_v \geq \alpha_{v2}^{\text{img}}\right)$$

OR

$$\text{Condition } 4.7 : \left(-\eta^2 < \kappa < 0\right)\text{AND}\left(\chi < -\frac{\kappa}{\eta}\right)\text{AND}\left(\alpha_v \geq \max\left\{\alpha_{v2}^{\text{img}}, \alpha_v^{\infty}\right\}\right)$$

OR

$$\text{Condition } 4.8 : \left(-\eta^2 < \kappa < 0\right)\text{AND}\left(-\frac{\kappa}{\eta} \leq \chi \leq -\frac{1}{\kappa\eta}\right)\text{AND}\left(\alpha_v \geq \alpha_v^{\infty}\right)$$

OR

$$\text{Condition } 4.9 : \left(-\eta^2 < \kappa < 0\right)\text{AND}\left(\chi > -\frac{1}{\kappa\eta}\right)\text{AND}\left(\alpha_v \leq \alpha_v^{\infty}\ \text{OR}\ \alpha_v \geq \alpha_{v2}^{\text{img}}\right)$$

OR

$$\text{Condition } 4.10 : (\kappa > 0)\text{AND}\left(\alpha_v \geq \alpha_v^{\infty}\right)$$

Each sufficient condition in **Result 4** is derived from the negative zero loci in Fig. 1. For example, in Fig. 1a, when ($\kappa < -1$) AND ($\chi < -\eta^3/\kappa$), RNMP zeros are not part of the zero locus. Therefore, they do not occur for any value of α_v. CNMP zeros are part of the zero locus but they only occur when CMP zeros cross the imaginary axis for $\alpha_v < \alpha_{v2}^{\text{img}}$. This leads to Condition 4.1 for the elimination of all NMP zeros i.e. [($\kappa < -1$) AND ($\chi < -\eta^3/\kappa$) AND ($\alpha_v \geq \alpha_{v2}^{\text{img}}$)]. Similarly, other sufficient conditions are also derived from the negative zero loci of Fig. 1. The correspondence between each sufficient condition and Fig. 1 is as follows: Condition 4.1 → Fig. 1a, Condition 4.2 → Fig. 1b-1e, Condition 4.3 → Fig. 1f, Condition 4.4 → Fig. 1g, Condition 4.5 → Fig. 1h, Condition 4.6 → Fig. 1i, Condition 4.7 → Fig. 1j, Condition 4.8 → Fig. 1k-1n, Condition 4.9 → Fig. 1o, and Condition 4.10 → Fig. 1p.

Based on **Result 4** and Fig. 1, the following observations can be made about the NMP zero dynamics of a three-DoF damped flexible system:

1 The general observations made for **Result 3** above i.e. bullet point (1) to point (5) also hold true for **Result 4** when the modal residue signs are not alternating.

2 Condition 4.2 is the only condition that holds true for any negative value of modal residue α_v or any positive value of α_u and any positive value of modal damping ratio ζ_v or ζ_u. Therefore, such a condition becomes useful when the modal residue α_v or α_u and/or modal damping ratio ζ_v or ζ_u undergo large variations [12].

3 Condition 4.10 is the only condition that holds true for any value of modal damping ratios ζ_v and/or ζ_u. Therefore, such a condition becomes useful when modal damping ratios undergo large variations.

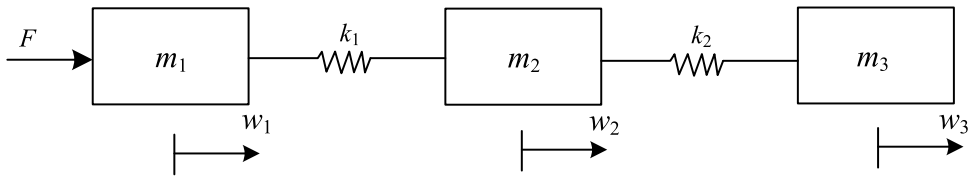

Fig. 2. Three-DoF Undamped Flexible System.

4. Case study of three-DoF flexible system

This section demonstrates how the results from Section 3 can be used to determine the location, value of viscous dampers and sensor placement in a three-DoF flexible system in order to eliminate NMP zeros in its transfer function and also place zeros on the imaginary axis. Furthermore, it will be demonstrated that the elimination of NMP zeros is robust to parametric variations in sensor placement.

Consider the three-DoF flexible system shown in Fig. 2. For illustration, the physical parameters of this system are chosen as $m_1 = m_3 = 1$ kg, $m_2 = 10$ kg, $k_1 = k_2 = 1$ N/m. The force, F is applied at m_1 and the measured displacement, q is the linear combination of the displacement of m_1 and m_3 i.e. $q = w_1 + 3w_3$. The equations of motion of the undamped three-DoF flexible system is given below.

$$[\mathbf{M}]\begin{bmatrix}\ddot{w}_1\\ \ddot{w}_2\\ \ddot{w}_3\end{bmatrix} + [\mathbf{K}]\begin{bmatrix}w_1\\ w_2\\ w_3\end{bmatrix} = [\mathbf{B}]F,\ q = [\mathbf{D}]\begin{bmatrix}w_1\\ w_2\\ w_3\end{bmatrix} \text{ where } [\mathbf{M}] = \begin{bmatrix}m_1 & 0 & 0\\ 0 & m_2 & 0\\ 0 & 0 & m_3\end{bmatrix},\ [\mathbf{K}] = \begin{bmatrix}k_1 & -k_1 & 0\\ -k_1 & k_1+k_2 & -k_2\\ 0 & -k_2 & k_2\end{bmatrix},\ [\mathbf{B}] = \begin{bmatrix}1\\ 0\\ 0\end{bmatrix} \tag{15}$$

$$[\mathbf{D}] = [\,1 \quad 0 \quad 3\,]$$

The transfer function from applied force, F to measured displacement, q is given below along with its poles and zeros.

$$\frac{q(s)}{F(s)} = \frac{s^4 + 1.2s^2 + 0.4}{s^6 + 2.2s^4 + 1.2s^2},\ \text{Poles}: p_{1,2} = 0,\ p_{3,4} = \pm 1j,\ p_{5,6} = \pm 1.1j,\ \text{Zeros}:\ z_{1,2,3,4} = \pm 0.127 \pm 0.785j \tag{16}$$

This system exhibits a CMP-CNMP zero quartet. Our goal is to add viscous damping (location and value) to the flexible system so as to eliminate NMP zeros from the transfer function. The equations of motion of the resulting three-DoF damped flexible system (Fig. 3) are given below.

$$[\mathbf{M}]\begin{bmatrix}\ddot{w}_1\\ \ddot{w}_2\\ \ddot{w}_3\end{bmatrix} + [\mathbf{C}]\begin{bmatrix}\dot{w}_1\\ \dot{w}_2\\ \dot{w}_3\end{bmatrix} + [\mathbf{K}]\begin{bmatrix}w_1\\ w_2\\ w_3\end{bmatrix} = [\mathbf{B}]F,\ q = [\mathbf{D}]\begin{bmatrix}w_1\\ w_2\\ w_3\end{bmatrix} \text{ where } [\mathbf{C}] = \begin{bmatrix}c_1+c_3 & -c_1 & -c_3\\ -c_1 & c_1+c_2 & -c_2\\ -c_3 & -c_2 & c_2+c_3\end{bmatrix} \tag{17}$$

In this paper, we have assumed that the flexible system is 'classically damped'. This means that the mass matrix [**M**], stiffness matrix [**K**], and damping matrix [**C**] should satisfy the Caughey and O'Kelly criterion given in Eq. (2), Section 2. Applying Eq. (2) to the [**M**], [**C**], and [**K**] from Eq. (17) and using the numerical values of $m_1 = m_3 = 1$ kg, $m_2 = 10$ kg, $k_1 = k_2 = 1$ N/m leads to the following condition on the viscous dampers c_1, c_2, and c_3.

$$\begin{aligned} &c_1 = c_2\\ &c_3 \text{ can be any arbitrary value}\end{aligned} \tag{18}$$

The result that c_3 can be any arbitrary value tells us that for any value of c_3, Eq. (2) is satisfied. Therefore, we choose $c_3 = 0$ to keep the ensuing mathematical analysis simple. Since, the Caughey and O'Kelly criterion is satisfied, the [**M**], [**C**], and [**K**] matrices can be simultaneously diagonalized to obtain the modal mass, modal damping and modal stiffness diagonal matrices as demonstrated in Eq. (3). The modal mass, damping and stiffness matrices are then used to construct the decomposed form of the transfer function as

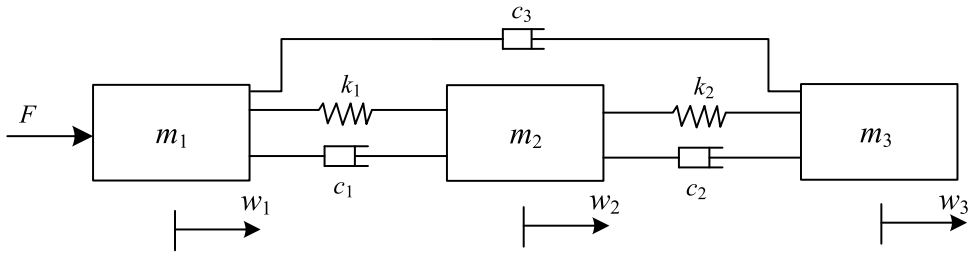

Fig. 3. Three-DoF Damped Flexible System.

demonstrated in Eq. (4) and Eq. (5). The decomposed transfer function in terms of the viscous damper, c_1 is given below. Note that from Eq. (18), we already know that $c_2 = c_1$ and we have chosen $c_3 = 0$.

$$\frac{q(s)}{F(s)} = \frac{\alpha_R}{s^2} + \frac{\alpha_u}{s^2 + 2\zeta_u\omega_u s + \omega_u^2} + \frac{\alpha_v}{s^2 + 2\zeta_v\omega_v s + \omega_v^2} = \frac{0.33}{s^2} + \frac{-1}{s^2 + c_1 s + 1} + \frac{1.67}{s^2 + 1.2c_1 s + 1.21} \tag{19}$$

Comparing the LHS and RHS of the Eq. (19) provides the relationship between c_1, ζ_u and ζ_v.

$$\zeta_u = 0.5c_1 \text{ and } \zeta_v = 0.547c_1 \tag{20}$$

The modal residue signs in Eq. (19) are alternating with $\alpha_v > 0$. According to Table 1, we should use **Result 3** to eliminate all NMP zeros in the transfer function with alternating modal residue signs. There are 9 distinct conditions in **Result 3** and we have to choose the appropriate condition for our current system. From Eq. (19), the value of κ, η and χ can be readily found as shown below. Since, both ζ_u and ζ_v are proportional to c_1, as evident in Eq. (20), their ratio i.e. χ is independent of it.

$$\kappa\left(\triangleq \frac{\alpha_u}{\alpha_v}\right) = -0.6, \eta\left(\triangleq \frac{\omega_u}{\omega_v}\right) = 0.91, \text{ and } \chi\left(\triangleq \frac{\zeta_u}{\zeta_v}\right) = 0.914 \tag{21}$$

Based on the values of κ, η and χ, it can be inferred that the following two inequalities are simultaneously satisfied.

$$\left(-\eta^2 < \kappa < 0\right) \text{AND} \left(-\frac{\kappa}{\eta} < \chi < -\frac{\eta^3}{\kappa}\right) \tag{22}$$

In **Result 3**, only Condition 3.7 and Condition 3.8 are applicable to our current system since they satisfy Eq. (22).

$$\begin{aligned} &\text{Condition 3.7}: \left(-\eta^2 < \kappa < 0\right) \text{AND} \left(-\frac{\kappa}{\eta} < \chi < -\frac{\eta^3}{\kappa}\right) \text{AND} (\zeta_v < \zeta_0) \text{AND} \left(\alpha_v \le \alpha_{v1}^{\text{img}} \text{ OR } \alpha_v \ge \alpha_{v2}^{\text{img}}\right) \\ &\text{OR} \\ &\text{Condition 3.8}: \left(-\eta^2 < \kappa < 0\right) \text{AND} \left(-\frac{\kappa}{\eta} < \chi < -\frac{\eta^3}{\kappa}\right) \text{AND} (\zeta_v \ge \zeta_0) \end{aligned} \tag{23}$$

In order to completely satisfy Condition 3.8, we only need to additionally satisfy $\zeta_v \ge \zeta_0$. This will give us the value of c_1 that will guarantee the elimination of NMP zeros in the transfer function in Eq. (19). However, in order to satisfy Condition 3.7, we will have to modify the value of α_v which can only done by modifying the mass matrix, stiffness matrix, actuator or sensor location. Since, our goal is to eliminate NMP zeros by simply adding viscous damping, we decide to satisfy Condition 3.8. Using the expression of ζ_0 from Eq. (14) along with the numerical value of κ, η and χ from Eq. (21) leads to the following result.

$$\zeta_v \ge 0.2350 \tag{24}$$

Eq. (20) is used along with Eq. (24) to find the range of values for c_1 for which the transfer function in Eq. (19) will not have any NMP zeros.

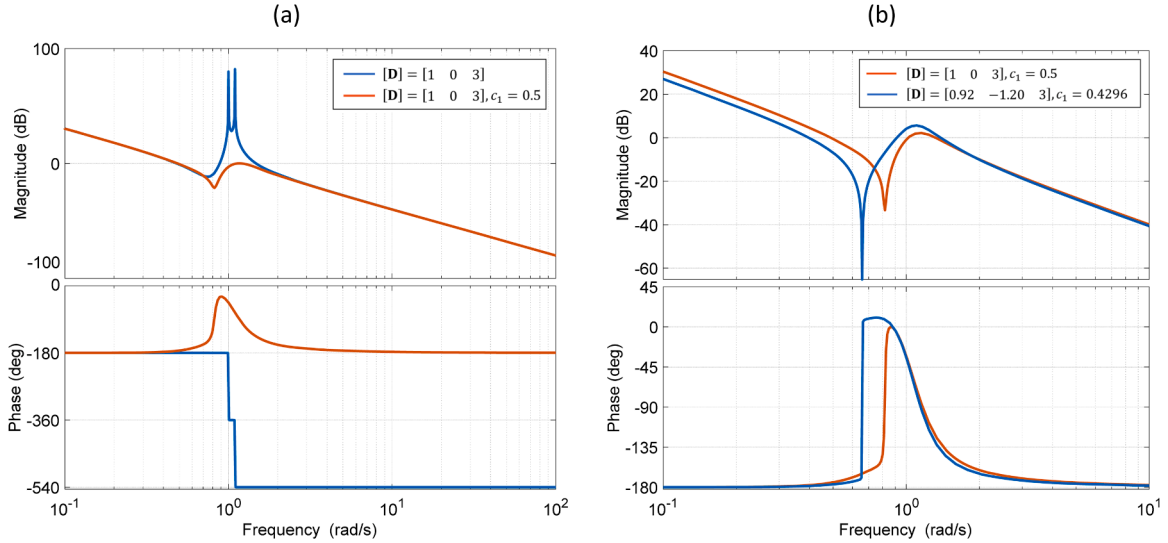

Fig. 4. Bode plots of: a) undamped vs. damped system with tuned damping to eliminate NMP zeros, b) damped system with tuned damping and sensor vector to place the zero on the imaginary axis.

$$c_1 \geq 0.4296 \tag{25}$$

Therefore, selecting $c_1 = c_2 = 0.5$ and $c_3 = 0$ leads to a transfer function of the three-DoF damped flexible system that does not exhibit any NMP zeros as shown below. Note that this transfer function is simply obtained by substituting $c_1 = 0.5$ in Eq. (19).

$$\begin{aligned} &\frac{q(s)}{F(s)} = \frac{s^4 + 0.6s^3 + 1.3s^2 + 0.4s + 0.4}{s^6 + 1.1s^3 + 2.5s^4 + 1.2s^3 + 1.2s^2} \\ &\text{Poles}: \ p_{1,2} = 0, p_{3,4} = -0.2500 \pm 0.9682j, p_{5,6} = -0.3000 \pm 1.0536j \\ &\text{Zeros}: \ z_{1,2} = -0.2700 \pm 0.7210j, \ z_{3,4} = -0.0300 \pm 0.8210j \end{aligned} \tag{26}$$

Since, the damped flexible system satisfies Condition 3.8, Fig. 1m (from which Condition 3.8 was derived) predicts that its transfer function will exhibit two pairs of CMP zeros. This is shown to be true in Eq. (26) where $z_{1,2}$ and $z_{3,4}$ denote the two CMP zero pairs. Not only that, one of the CMP zero pair i.e. $z_{1,2}$ is placed very close to the pole pair i.e. $p_{1,2}$ leading to approximate pole-zero cancelation and effectively eliminating any 'vibration' at the $p_{1,2}$ frequency. The other CMP zero pair i.e. $z_{3,4}$ is located very close to the imaginary axis leading to improved 'vibration isolation' at its frequency. This improvement in the 'vibration performance' of the damped system achieved via the elimination of NMP zeros is shown via a Bode plot in Fig. 4a.

Note that the zero pair $z_{3,4}$ is not exactly located on the imaginary axis. If further 'vibration isolation' is desired by placing $z_{3,4}$ exactly on the imaginary axis, it can also be easily achieved based on the graphical insight obtained from Fig. 1l. According to the positive zero locus in Fig. 1l, if $(\zeta_v = \zeta_0)$ AND $(\alpha_v = \alpha_{v1}{}^{\text{img}} = \alpha_{v2}{}^{\text{img}})$ are satisfied, then $z_{3,4}$ will lie exactly on the imaginary axis. In order to satisfy $(\zeta_v = \zeta_0)$, choose $c_1 = 0.4296$ (see Eq. (24) and Eq. (25)). Choosing $(\zeta_v = \zeta_0)$ automatically ensure that $\alpha_{v1}{}^{\text{img}} = \alpha_{v2}{}^{\text{img}}$ (see Fig. 1l). Finally, $\alpha_v = \alpha_{v1}{}^{\text{img}}$ can be ensured by modifying the value of α_v. One of the ways to modify the value of α_v is by altering the sensor vector **[D]**, which is parameterized as follows.

$$[\mathrm{D}] = [\,1 + \varepsilon_1 \quad \varepsilon_2 \quad 3\,] \tag{27}$$

The value of ε_1 and ε_2 is found by using the relationship between α_v and **[D]**, given in Eq. (5), and imposing the two conditions shown below. The condition on $\kappa\,(= \alpha_u / \alpha_v)$ is to make sure that value of ζ_0 and $\alpha_{v1}{}^{\text{img}}$ that were calculated for a constant $\kappa = -0.6$ (Eq. (21)) do not change as α_v is changed.

$$\left(\alpha_v = \alpha_{v1}^{\text{img}}\right) \text{AND} (\kappa = -0.6) \tag{28}$$

Solving the conditions in Eq. (28) for the two unknowns ε_1 and ε_2 leads to the following sensor vector.

$$[\mathrm{D}] = [\,0.92 \quad -1.2 \quad 3\,] \tag{29}$$

The zeros of the transfer function $q(s)$ / $F(s)$ with the new sensor vector from Eq. (29) and $c_1 = 0.4296$ are as follows:

$$z_{1,2} = -0.2674 \pm 0.7801j, \ z_{3,4} = \pm 0.6590j \tag{30}$$

It can be clearly seen that the zero pair $z_{3,4}$ is now on the imaginary axis as intended. The ensuing improvement in vibration isolation due to the tuning of the viscous damper c_1 and sensor vector **[D]** is shown via a Bode plot in Fig. 4b. Therefore, by informed choice of the damping matrix **[C]** and sensor vector **[D]**, the CNMP zeros of the three-DoF *undamped* flexible system can be converted into MP zeros of its *damped* counterpart lying exactly on the imaginary axis.

To investigate the robustness of the damped system obtained using the proposed technique for a fixed c_1 that satisfies Eq. (25), Bode

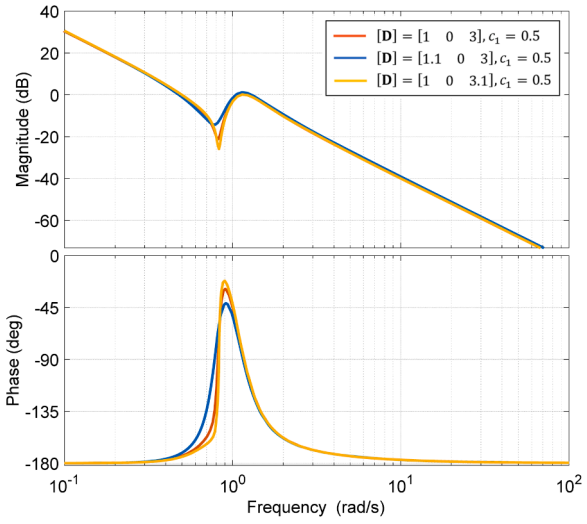

Fig. 5. Robust elimination of NMP zeros under variation in sensor vector.

plots of the damped system with variations in the sensor vector [**D**] are shown in Fig. 5. Variation in the sensor vector is generally caused by uncertainty in sensor placement. It can be observed from the Bode plots that even in the presence of finite perturbations (up to 10%) in the sensor parameters, the designed damping matrix [**C**] still ensures that all the zeros of the flexible system remain MP. This is because even in the presence of this sensor parameter variation, the inequalities in Condition 3.8 are still satisfied. It should be noted that this level of robustness exists for $c_1 = c_2 = 0.5$, which is very close to the minimum required value of damping given in Eq. (25). If a more robust design is needed for a given application, then larger damping values can be chosen to ensure an even wider safety margin. Thus, this case study highlights that the new sufficient and necessary conditions derived in Section 3 of this paper can be effectively used to enable *robust physical design* of three-DoF flexible systems.

5. Conclusion and future work

In this paper, the sufficient and necessary conditions for the elimination of NMP zeros in a three-DoF classically damped flexible LTI system (with one rigid body mode and two flexible modes) are presented when all the modal residue signs are not same. No such results exist in the prior literature.

Results 3 and **4** provide a *complete set* of all possible sufficient conditions for the elimination of all NMP zeros. This *complete set* of sufficient conditions when imposed together also becomes the necessary condition for the elimination of NMP zeros. These conditions enable informed physical design choices such as selection of viscous damping strategies and values, actuator and sensor placement, mass and stiffness distribution, etc. These choices can lead to robust physical design that guarantees the elimination of NMP zeros over a wide range of system parameters, as shown via a case study.

While the results of this paper are novel, the mathematical and graphical tools used are not necessarily unique. But these tools allow one to derive conditions for the elimination of *specific* types of zeros as well as provide graphical insights into the behavior of the zeros as system parameters are varied. For example, **Results 1** and **2** provide sufficient conditions for elimination of specifically CNMP zeros, which are relevant to certain classes of flexible systems that only exhibit CNMP zeros [36]. Furthermore, the graphical insights offered by the zero loci allow one to examine the robustness of the zero dynamics to parametric variations i.e. how close the minimum phase zeros are to the imaginary axis and when they might transition to non-minimum phase.

While we investigated three-DoF damped flexible systems here, our future work focuses on deriving analytical conditions to eliminate NMP zeros in multi-DoF damped flexible systems. To do so, we are currently investigating techniques to reduce the size of the parameter space of an *n*-DoF damped flexible system from *3n* system parameters to fewer composite parameters.

Credit author statement

Siddharth Rath is a Ph.D. candidate in Mechanical Engineering at the University of Michigan, Ann Arbor. Dr. Shorya Awtar is a Professor of Mechanical Engineering and his Ph.D. advisor.

Both authors have contributed equally to the intellectual contents of this manuscript, along with its overall writing, presentation, tables, and figures.

Declaration of Competing Interest

None.

Data availability

No data was used for the research described in the article.

Acknowledgement

This work was supported in part by a National Science Foundation Grant (CMMI # 1941194).

References

[1] S.D. Gennaro, Output stabilization of flexible spacecraft with active vibration suppression, IEEE Trans. Aerosp. Electron. Syst. 39 (3) (2003) 747–759.
[2] P.C. Hughes, Dynamics of flexible space vehicles with active attitude control, Celest. Mech. 9 (1) (1974) 21–39.
[3] P.P. Friedmann, T.A. Millott, Vibration reduction in rotorcraft using active control - a comparison of various approaches, J. Guid Control Dyn. 18 (4) (1995) 664–673.
[4] M.M. Uddin, P. Sarker, C.R. Theodore, U.K. Chakravarty, Active vibration control of a helicopter rotor blade by using a linear quadratic regulator, ASME Int. Mech. Eng. Congress Expos. 52002 (2018). V001T03A014.
[5] J.Y. Chang, Hard disk drive seek-arrival vibration reduction with parametric damped flexible printed circuits, Microsyst. Technol. 13 (8) (2007) 1103–1106.
[6] G. Feng, Y. Fook Fah, Y. Ying, Modeling of hard disk drives for vibration analysis using a flexible multibody dynamics formulation, IEEE Trans. Magn. 41 (2) (2005) 744–749.
[7] S. Awtar, G. Parmar, Design of a large range XY nanopositioning system, J. Mech. Robot. 5 (2) (2013), 021008.
[8] N.K. Roy, M.A. Cullinan, Design and characterization of a two-axis, flexure-based nanopositioning stage with 50 mm travel and reduced higher order modes, Precision Eng. 53 (2018) 236–247.
[9] N.G. Chalhoub, A.G. Ulsoy, Dynamic simulation of a leadscrew driven flexible robot arm and controller, J. Dyn. Syst. Meas. Control 108 (2) (1986) 119–126.

[10] K.K. Varanasi, S.A. Nayfeh, The dynamics of lead-screw drives: low-order modeling and experiments, J. Dyn. Syst. Meas. Control 126 (2) (2004) 388–396.
[11] L. Cui, S. Awtar, Experimental validation of complex non-minimum phase zeros in a flexure mechanism, Precision Eng. 60 (2019) 167–177.
[12] L. Cui, C. Okwudire, S. Awtar, Modeling complex nonminimum phase zeros in flexure mechanisms, J. Dyn. Syst. Meas. Control 139 (10) (2017), 101001.
[13] N. Loix, J. Kozanek, E. Foltete, On the complex zeros of non-colocated systems, J. Struct. Control 3 (1–2) (1996) 79–87.
[14] R.H. Cannon, E. Schmitz, Initial experiments on the end-point control of a flexible one-link robot, Int. J. Rob. Res. 3 (3) (1984) 62–75.
[15] J. Freudenberg, D. Looze, Right half plane poles and zeros and design tradeoffs in feedback systems, IEEE Trans. Automat. Contr. 30 (6) (1985) 555–565.
[16] M. Kamaldar, S.A.U. Islam, J.B. Hoagg, D.S. Bernstein, Demystifying enigmatic undershoot in setpoint command following [Focus on Education], IEEE Control Syst. Mag. 42 (1) (2022) 103–125.
[17] L. Cui, "On the Complex Non-Minimum Phase Zeros in Flexure Mechanism," Ph.D. dissertation, University of Michigan, Ann Arbor, MI, 2017.
[18] O.O. Bendiksen, Mode localization phenomena in large space structures, AIAA J. 25 (9) (1987) 1241–1248.
[19] D. Afolabi, B. Alabi, Catastrophe theory, curve veering and the vibration of bladed discs, Proc. Inst. Mech. Eng., Part C 206 (2) (1992) 143–144.
[20] M.P. Castanier, C. Pierre, Modeling and analysis of mistuned bladed disk vibration: current status and emerging directions, J. Propul. Power 22 (2) (2006) 384–396.
[21] J.E. Mottershead, Complex and defective zeros in cross receptances, J. Sound Vib. 246 (1) (2001) 190–197.
[22] J. Mottershead, Structural modification for the assignment of zeros using measured receptances, J. Appl. Mech. 68 (5) (2001) 791–798.
[23] J.E. Mottershead, C. Mares, M.I. Friswell, An inverse method for the assignment of vibration nodes, Mech. Syst. Signal Process. 15 (1) (2001) 87–100.
[24] S. Rath, L. Cui, S. Awtar, On the zeros of an undamped three-DOF flexible system, ASME Lett. Dyn. Syst. Control 1 (4) (2021), 041010.
[25] H. Pierson, J. Brevick, K. Hubbard, The effect of discrete viscous damping on the transverse vibration of beams, J. Sound Vib. 332 (18) (2013) 4045–4053.
[26] K.K. Varanasi, S.A. Nayfeh, Damping of flexural vibration using low-density, low-wave-speed media, J. Sound Vib. 292 (1) (2006) 402–414.
[27] J.A. Main, S. Krenk, Efficiency and tuning of viscous dampers on discrete systems, J. Sound Vib. 286 (1) (2005) 97–122.
[28] H.T. Banks, D.J. Inman, On damping mechanisms in beams, J. Appl. Mech. 58 (3) (1991) 716–723.
[29] K.A. Morris, M. Vidyasagar, A comparison of different models for beam vibrations from the standpoint of control design, J. Dyn. Syst. Meas. Control 112 (3) (1990) 349–356.
[30] A.G. Thompson, Optimum tuning and damping of a dynamic vibration absorber applied to a force excited and damped primary system, J. Sound Vib. 77 (3) (1981) 403–415.
[31] N. Hoffmann, L. Gaul, Effects of damping on mode-coupling instability in friction induced oscillations, J. Appl. Math. Mech. 83 (2003) 524–534.
[32] C.T. Sun, J.M. Bai, Vibration of multi-degree-of-freedom systems with non-proportional viscous damping, Int. J. Mech. Sci. 37 (4) (1995) 441–455.
[33] S.T. Pang, T. Tsao, L.A. Bergman, Active and passive damping of euler-bernoulli beams and their interactions, J. Dyn. Syst. Meas. Control 115 (3) (1993) 379–384.
[34] A.E. Thomas, S.L. Dickerson, B.J. Wayne, On the transfer function modeling of flexible structures with distributed damping, in: ASME Winter Annual Meeting, 1986, pp. 23–30.
[35] P. Duffour, J. Woodhouse, Instability of systems with a frictional point contact. Part 1: basic modelling, J. Sound Vib. 271 (1–2) (2004) 365–390.
[36] J.B. Hoagg, J. Chandrasekar, D.S. Bernstein, On the zeros, initial undershoot, and relative degree of collinear lumped-parameter structures, J. Dyn. Syst. Meas. Control 129 (4) (2006) 493–502.
[37] J.L. Lin, J.N. Juang, Sufficient conditions for minimum-phase second-order linear systems, J. Vib. Control 1 (2) (1995) 183–199.
[38] J.L. Lin, On Transmission Zeros of Mass-Dashpot-Spring Systems, J. Dyn. Syst. Meas. Control 121 (2) (1999) 179–183.
[39] T. Williams, Transmission-zero bounds for large space structures, with applications, J. Guid. Control Dyn. 12 (1) (1989) 33–38.
[40] S. Rath, S. Awtar, Non-minimum phase zeros of two-DoF damped flexible systems, in: Modelling, Estimation and Control Conference, Austin, Texas 54, 2021, pp. 579–585. October 24-27.
[41] M. Tohyama, R.H. Lyon, Zeros of a transfer function in a multi-degree-of-freedom vibrating system, J. Acoust. Soc. Am. 86 (5) (1989) 1854–1863.
[42] M. Tohyama, Room Transfer Function. Handbook of Signal Processing in Acoustics, 2008, pp. 1381–1402.
[43] J.M. Roesset, R.V. Whitman, R. Dobry, Modal analysis for structures with foundation interaction, J. Struct. Div. 99 (3) (1973) 399–416.
[44] N.C. Tsai, Modal damping for soil-structure interaction, J. Eng. Mech. Div. 100 (2) (1974) 323–341.
[45] W.T. Thomson, T. Calkins, P. Caravani, A numerical study of damping, Earthquake Eng. Struct. Dyn. 3 (1) (1974) 97–103.
[46] T.K. Caughey, M.E.J. O'Kelly, Classical normal modes in damped linear dynamic systems, J. Appl. Mech. 32 (3) (1965) 583–588.
[47] L. Meirovitch, Analytical Methods in Vibration, 19, The Macmillan Company, New York, 1967.
[48] S. Rath, "On the Zeros of Flexible Systems," Ph.D. dissertation, University of Michigan, Ann Arbor, MI, 2023.